AB INITIO STUDIES OF COMPOUND SEMICONDUCTOR SURFACES

Tapio T. RANTALA
Department of Physical Sciences, University of Oulu,
P.O.Box 333, FIN-90571 Oulu, Finland.
E-mail: Tapio.Rantala@oulu.fi

A brief review of compound semiconductor surface structures and properties studied with *ab initio* methods is given. First, the methodology based on the density-functional formalism and local-density approximation is described, followed by a description of two alternative computational techniques. Then, two chosen semiconductor surfaces are considered as examples, the $(10\bar{1}0)$ face of a tetrahedrally bonded CdS and the (110) face of a rutile SnO_2. Also, some aspects of the surface chemical activity are discussed.

1 Introduction

Compound semiconductors offer a multitude of possibilities for designing new materials. The number of possible binary compounds formed from the elements of main groups from II to VII is very large, already, let alone the combinations of more than two components. Furthermore, doping and use of layered structures allows one to tune the electrical and optical properties of semiconductor materials at will. A play with crystalline, layered, amorphous and porous materials allows one to select the mechanical and chemical properties, too. In all, both the bulk properties and surface chemical activity of compound semiconductors can be engineered, if the underlying principles and origin of the properties are sufficiently well known. It is this expertise where the theoretical and computational research can contribute most.

It is the surface of solid materials, where the contact and interaction with the environment of a piece of matter takes place. It makes the surface properties of materials of essential importance. Until lately, the main focus of attention in surface science has mostly been in research of simple metal and other elemental surfaces. Though, it has given us much insight to surface phenomena, adsorption, surface diffusion, catalyzed reactions, etc., there still remain details to be uncovered. This is true with complex compound materials, in particular. On the other hand, as pointed out above the compound materials offer good possibilities for materials engineering. This motivates the computational (and experimental) studies of compound semiconductor surfaces, in general,[1–7] and in such new applications as gas sensors,[1,2] in particular.

In this text we first present the density-functional formalism, which is

the basis of the applied *ab initio* methods in our studies. Next, the two applied computational techniques, one based on the linear-combination-of-atomic-orbitals (LCAO) and the other employing plane waves and pseudopotentials (PWPP) are described. We aim at giving a relatively complete account of these matters with as simple concepts as possible. Therefore, we start from basics but include only the most essential concepts and try to keep the text easy to read. Then, the use of these computational techniques is demonstrated in the subsequent two case studies. Relaxation of the chosen cleavage surfaces of tetrahedrally bonded CdS and rutile structure metal oxide SnO_2 are considered. Some aspects of the surface chemical activity are discussed, too.

2 First Principles Approach

2.1 Many-electron Problem

The vast majority of the properties of matter depend on its electronic structure, the quantum state of the electrons involved. The electrons bind the atoms to molecules or solids and they are responsible for most of the interactions between pieces of matter. Furthermore, it is also the electrons that respond to many external perturbations of matter, e.g. irradiation. The main job left for the atomic nuclei is to provide the charge balancing environment for the electrons to move, but the conformation and dynamics of nuclei, on the other hand, follow the force field given by the electronic structure. It is this interplay between electrons and nuclei that is responsible for the surface chemistry, thermal properties and many other bulk properties of solids. Therefore, we are interested in computationally searching for the properties and dynamics of a system of electrons and nuclei.

The stationary quantum state of the many-particle system (here, electrons and nuclei) is a solution to the Schrödinger equation

$$H\Psi = E\Psi, \tag{1}$$

where the hamiltonian H includes all of the Coulomb pair interactions and the kinetic energies of all particles in the system. The total energy of the system E is obtained as an eigenvalue associated to the wavefunction Ψ. This solution, in principle, provides us with all the information we may wish.

In what follows we do not treat nuclear dynamics quantum mechanically and we limit us to the non-relativistic treatment. Furthermore, the spin of the electrons is not treated explicitly. Thus, the N-electron hamiltonian in the

surroundings of M atomic nuclei reads (in atomic units) as

$$H = \sum_{i}^{N} \left(-\frac{1}{2}\nabla_i^2 + v_{\mathrm{ne}}(\mathbf{r}_i) \right) + \sum_{i<j}^{N,N} \frac{1}{r_{ij}} + V_{\mathrm{nn}}, \tag{2}$$

where

$$v_{\mathrm{ne}}(\mathbf{r}_i) = \sum_{\mu}^{M} \left(-\frac{Z_\mu}{r_{i\mu}} \right), \quad V_{\mathrm{nn}} = \sum_{\mu<\nu}^{M,M} \frac{Z_\mu Z_\nu}{R_{\mu\nu}}, \tag{3}$$

$r_{i\mu} = |\mathbf{r}_i - \mathbf{R}_\mu|$, $r_{ij} = |\mathbf{r}_i - \mathbf{r}_j|$, $R_{\mu\nu} = |\mathbf{R}_\mu - \mathbf{R}_\nu|$ and Z_μ are the nuclear charges. The two terms, $v_{\mathrm{ne}}(\mathbf{r})$ and V_{nn}, Eqs. 3, are the Coulomb potential energy of electrons in the field of nuclei and the mutual Coulomb repulsion energy of nuclei, respectively. They depend on the set of electronic coordinates $\{\mathbf{r}_i\}$ and the set of nuclear coordinates $\{\mathbf{R}_\mu\}$.

It should be noted that it is the nuclear conformation $\{\mathbf{R}_\mu\}$, nuclear charges $\{Z_\mu\}$ and the number of electrons N that suffice to specify the whole quantum state of the electronic system. The calculation procedures which start with this least possible information about the system and use only principles of quantum theory are called *ab initio* or "first principles" methods. Basically both of these terms mean the same concept, though some authors have assigned them to some specific calculation procedures, too.

The solution to the Eq. 1 should provide us with data to compare with the related experiments, and concepts for obtaining physical insight to the system. For these reasons it is helpful to decompose the complex many-electron system (or state) to one-electron states, and correspondingly, describe the many-electron quantities, like total energy, with contributions of single electron states. In fact, the standard solution procedures start with this s.c. one-electron picture: mutually interacting electrons in their own separable eigenstates. These eigenstates ψ_i are solutions to their one-electron Schrödinger equations

$$h_i(\mathbf{r}_i)\,\psi_i(\mathbf{r}_i) = \varepsilon_i\,\psi_i(\mathbf{r}_i). \tag{4}$$

There are two conventional *ab initio* approaches to solve Eq. 1 for Ψ, the wavefunction formalism and the density-functional formalism. The wavefunction formalism starts with the one-electron spin-orbitals ψ_i of the electrons in the system. An antisymmetrized product of spin-orbitals Ψ^{HF}, e.g. a Slater determinant,[8] and the variational total energy minimization leads to a set of one-electron equations of the form of Eq. 4. These are s.c. Hartree–Fock equations, where h_i is called the Fock operator.[8,9] The antisymmetric Hartree–Fock wavefunction Ψ^{HF} includes the exchange interaction of electrons but does not take into account all details of the mutual Coulomb correlations of electrons

resulting from the interaction term $\sum_{i<j} 1/r_{ij}$. This deficiency is a limitation of the one-electron picture and it is usually corrected with s.c. "configuration interaction" or "multiconfiguration" scheme, where the correlated wavefunction Ψ^{CI} is written as a linear combination of the ground state and a large number of different excited state Hartree–Fock wavefunctions Ψ^{HF}.

The configuration interaction method offers, in principle, a systematic procedure to the solution of arbitrary high accuracy. However, as the system size or the number of electrons N increases the computational labor, increasing as N^3, soon becomes intolerable. This is due to the increasing number of electron–electron interaction integrals. Furthermore, with infinite systems like solids more fundamental problems arise. The long range of Coulomb interaction of electrons leads to unphysical singularities, unless an additional screening is included into the Hartree–Fock formalism.[10]

In the next section we introduce the other formalism, which circumvents many of these problems with a trade off of losing some of the accuracy. Nevertheless, it is better suited for the treatment of large and infinite system like crystals and surfaces. For finite systems, for example, the computational labor increases only linearly with respect to the number of electrons N.

2.2 Density-functional Formalism

The density-functional theory (DFT) is the other conventional *ab initio* approach to search for a solution to the many-electron Schrödinger equation, Eq. 1. A similar one-electron picture is invoked but the exchange and correlation of electrons is treated differently. Within DFT, the description is based on the electron density of the many-electron system. This is convenient, because the electron density is a well-defined measurable physical quantity and becomes even more relevant as the system size becomes larger. However, it should be kept in mind that the DFT is based on the very same physical preassumptions and first principles as the wavefunction formalism.

The starting point of DFT is the first Hohenberg–Kohn theorem,[11] which says that the external potential is determined, within a constant, by the electron density. This implies that there is one-to-one correspondence between the external potential of electrons $v_{\mathrm{ne}}(\mathbf{r})$, Eq. 3, and the ground state one-electron density $\rho(\mathbf{r})$ for a fixed number of electrons N. As the external potential $v_{\mathrm{ne}}(\mathbf{r})$ in the hamiltonian, Eq. 2, determines the many-electron wavefunction $\Psi(\{\mathbf{r}_i\})$ of Eq. 1, it follows that the one-to-one correspondence extends to the normalized $\Psi(\{\mathbf{r}_i\})$, too. Thus, all the ground state properties of a many-electron system are specified by its ground state one-electron density $\rho(\mathbf{r})$. Note that this is not restricted to Coulomb potentials, only.

Now, for a certain external potential $v_{\mathrm{ne}}(\mathbf{r})$, we can write the total energy of a many-electron system as a functional of its electron density and decompose it formally as

$$E[\rho] = T[\rho] + V_{\mathrm{ne}}[\rho] + V_{\mathrm{ee}}[\rho]. \tag{5}$$

The first term $T[\rho]$ is the kinetic energy of electrons, the second term

$$V_{\mathrm{ne}}[\rho] = \int \rho(\mathbf{r})\, v_{\mathrm{ne}}(\mathbf{r})\, \mathrm{d}\mathbf{r}, \tag{6}$$

is the Coulomb energy of charge density $\rho(\mathbf{r})$ in the external potential $v_{\mathrm{ne}}(\mathbf{r})$ and the third term $V_{\mathrm{ee}}[\rho]$ covers all the electron–electron interactions.

Application of the variational principle to the total energy functional $E[\rho]$ with respect to the function ρ proves the second Hohenberg–Kohn theorem: [11] the total energy is stationary at the ground state density with the energy E_0, or

$$E_0 \leq E[\rho]. \tag{7}$$

Thus, it has been demonstrated that solving the N electron problem for E_0 is equivalent with minimizing the total energy functional with respect to the electron density or with searching for the ground state density $\rho(\mathbf{r})$.

Again, a convenient practical approach [12] to search for $\rho(\mathbf{r})$ starts with writing it in terms of non-interacting one-electron states $\psi_i(\mathbf{r})$, for which

$$\rho(\mathbf{r}) = \sum_i^N \langle\psi_i|\psi_i\rangle = \sum_i^N |\psi_i(\mathbf{r})|^2 \tag{8}$$

and $\int \rho(\mathbf{r})\mathrm{d}\mathbf{r} = N$. Hence, we can write

$$T[\rho] = \sum_i^N \langle\psi_i|(-\frac{1}{2}\nabla_i^2)|\psi_i\rangle, \tag{9}$$

$$V_{\mathrm{ne}}[\rho] = \sum_i^N \langle\psi_i|v_{\mathrm{ne}}|\psi_i\rangle \tag{10}$$

and

$$V_{\mathrm{ee}}[\rho] = \frac{1}{2}\sum_i^N \langle\psi_i|v_{\mathrm{H}}|\psi_i\rangle + E_{\mathrm{xc}}[\rho]. \tag{11}$$

Here, the Hartree potential is

$$v_{\mathrm{H}}(\mathbf{r}) = \int \frac{\rho(\mathbf{r}')}{|\mathbf{r}-\mathbf{r}'|}\mathrm{d}\mathbf{r}', \tag{12}$$

which gives the larger term at the right hand side of Eq. 11, the classical Coulomb repulsion energy of the charge density $\rho(\mathbf{r})$, itself. The smaller contribution, the exchange and correlation energy, can formally be decomposed to the respective terms as

$$E_{\mathrm{xc}}[\rho] = E_{\mathrm{x}}[\rho] + E_{\mathrm{c}}[\rho]. \tag{13}$$

These terms contain all of the remaining electron–electron interactions beyond the Hartree energy.

Now, using the variational principle to the energy expression Eq. 5 written in terms of the orbitals ψ_i, one can derive[12] one-electron equations of the form of Eq. 4,

$$h_i(\mathbf{r}_i)\,\psi_i(\mathbf{r}_i) = \varepsilon_i \psi_i(\mathbf{r}_i). \tag{14}$$

These are called Kohn–Sham equations,[12,13] which are in the same role in DFT as the Hartree–Fock equations are in the wavefunction theory.

From Eqs. 9–11 it is relatively easy to inspect what the one-electron hamiltonian of the Kohn–Sham equations becomes to. It can be written as

$$h_i(\mathbf{r}_i) = -\frac{1}{2}\nabla_i^2 + v_{\mathrm{eff}}(\mathbf{r}_i), \tag{15}$$

where the effective one-electron potential is

$$v_{\mathrm{eff}}(\mathbf{r}) = v_{\mathrm{ne}}(\mathbf{r}) + v_{\mathrm{H}}(\mathbf{r}) + v_{\mathrm{xc}}(\mathbf{r}) \tag{16}$$

and further,

$$v_{\mathrm{xc}}(\mathbf{r}) = \frac{\delta E_{\mathrm{xc}}[\rho(\mathbf{r})]}{\delta \rho} \tag{17}$$

is sc. exchange–correlation potential. Solutions ψ_i to the Eq. 14 should be self-consistent, because the one-electron hamiltonian depends on the potential $v_{\mathrm{ee}}(\mathbf{r}) = v_{\mathrm{H}}(\mathbf{r}) + v_{\mathrm{xc}}(\mathbf{r})$, which depends on $\rho(\mathbf{r})$ written in terms of $\{\psi_i\}$.

Note that in writing the one-electron equations we have not done any approximations to the exact DFT, so far, and we are dealing with electrons whose all interactions are included in a functional of ρ, the effective potential $v_{\mathrm{eff}}(\mathbf{r})$, Eq. 16. This can be contrasted with the more complex Hartree–Fock equations of the wavefunction theory, which however, are known to describe an approximation including only the exchange but excluding the correlation interactions. In fact, the correlation interactions of electrons are usually defined to be those which are not described within the Hartree–Fock theory. Of course, things are not that simple with the DFT, either. The problems are just swept under the carpet for the present, i.e., the more complex interactions are gathered into

the exchange–correlation potential $v_{\mathrm{xc}}(\mathbf{r})$. It looks simple, it is just a function of $\mathbf{r}$ (for a fixed ρ) and even known exactly for the uniform electron density (for practical purposes). However, for the general case, non-uniform densities of atoms, molecules or solids, there are just various levels approximations of v_{xc} to choose from, so far.

The simplest approximations to the exchange–correlation potential v_{xc} and the corresponding energy per electron $\varepsilon_{\mathrm{xc}}$ are based on the properties of uniform electron gas. As mentioned above, for practical purposes these properties are known accurately enough from the Monte Carlo simulations of Ceperley and Alder.[14] In such case the constant density ρ or $r_s = (3/4\pi\rho)^{1/3}$ is the only parameter describing the whole system, if retaining to the spin-restricted case, only. Now, consider an electron gas with slow spatial variations, where we could expect the local properties of the electron gas to vary slowly, too. We could further expect that these properties depend almost entirely on the local electron density, not differing essentially from the properties of the uniform electron gas with the same density.

The slow spatial variations is the idea behind the local-density approximation (LDA), where the functional $v_{\mathrm{xc}}[\rho]$ defined in Eq. 17 is replaced by a local function $v_{\mathrm{xc}}^{\mathrm{LDA}}(\rho(\mathbf{r}))$. With the same approximation to the exchange and correlation energy per electron $\varepsilon_{\mathrm{xc}}^{\mathrm{LDA}}(\rho(\mathbf{r}))$ the exchange and correlation energy of the density $\rho(\mathbf{r})$ can be approximated with a simple integral

$$E_{\mathrm{xc}}^{\mathrm{LDA}} = \int \rho(\mathbf{r})\, \varepsilon_{\mathrm{xc}}^{\mathrm{LDA}}(\rho(\mathbf{r}))\, \mathrm{d}\mathbf{r}. \tag{18}$$

For practical calculations there are parameterized formulae fitted to the Monte Carlo data of the homogeneous electron gas.[13–16]

The LDA works well for solid materials,[15–18] especially for metals, and it has proven to be surprisingly successful even in cases where the density variations are relatively large like in free atoms and molecules.[13] The general experience is that LDA is good in predicting bond lengths and conformations, forces on atoms and vibrational frequencies, and general trends in chemistry. On the other hand, LDA fails in predicting bond energies accurately, and nonbonding interactions, and it systematically underestimates the band gap of semiconductors.

The most popular methods to improve LDA are based on sc. generalized gradient approximation [19] (GGA), where the effects of local density variations are described by density gradients and parameterized accordingly. The GGA is known to improve calculated total energies, atomization energies, energy barriers and the band gaps of semiconductors, though not always sufficiently. There are also methods [20] that do even better with these properties, especially

with the band gap problem, but are relatively heavy in practical computations.

From comparison of the results of DFT and wavefunction methods one can conclude that generally LDA does better than Hartree-Fock for the molecular properties.[13,19] However, where computationally feasible, i.e. for small molecules, the highly correlated wavefunction methods are the most accurate. For solids, on the other hand, the DFT method is the only applicable choice, in practice.

3 Computational Methods

3.1 LCAO Method

The one-electron states or orbitals of electrons are most conveniently solved as an expansion of suitable basis functions. Only spherically symmetric free atoms make an exception for which other numerical techniques are usually adopted. The set of basis functions can be chosen to suit best for the system in question. For small or disorderd structures with localized characteristics a set of atomic orbitals expanded around the nuclei may be the best choice, whereas for periodic bulk or other infinite structures plane waves may serve better. In this section, we first consider the common technique of using a set of localized basis functions, and in the next section, we consider the use of plane waves as basis functions.

The linear-combination-of-atomic-orbitals (LCAO) is the general name for methods where molecular orbitals or one-electron states ψ_i are expanded in terms of atomic one-electron orbitals $\{\varphi_{\mu k}\}$ centered around the nuclei at $\mathbf{R}_\mu$. The atomic orbitals can be written as

$$\varphi_{\mu k}(\mathbf{r}) = u_{n\ell}(r_\mu)\; Y_{\ell m_\ell}(\hat{\mathbf{r}}_\mu), \tag{19}$$

where $u_{n\ell}(r)$ is the radial part of the atomic orbital and $Y_{\ell m_\ell}(\hat{\mathbf{r}})$ is the angular part, the spherical harmonic function. Here $\mathbf{r}_\mu = \mathbf{r} - \mathbf{R}_\mu$, $r_\mu = |\mathbf{r}_\mu|$ and $\hat{\mathbf{r}} = (\theta, \phi)$, the angles of the polar coordinate representation of $\mathbf{r}$. The subscript k stands for the set of orbital quantum numbers $\{n, \ell, m_\ell\}$. Instead of the complex spherical harmonics the real combinations can be taken with the advantage of better suitability for describing bonding between atoms. For example, the combinations $Y_x = Y_{1,-1} - Y_{1,+1}$, $Y_y = Y_{1,-1} + iY_{1,+1}$ and $Y_z = Y_{1,0}$ are real functions for p-orbitals and conveniently oriented in space.

There are several forms in which the radial part of atomic type basis functions $u_{n\ell}(r_\mu)$ have conventionally been written for the computational use. The gaussian type orbitals (GTO) are composed as a sum of primitives, $u(r) = \sum_i b_i \exp(-\alpha_i r^2)$, which have convenient analytical properties. The Slater type orbitals (STO), usually scaled hydrogen like orbitals, have more realistic

functional form but they are less convenient in analytical calculations. One more practical alternative is the use of numerically calculated atomic orbitals of free atoms and ions. This is the choice that can be kept in mind when reading what follows.

The one-electron molecular orbitals are expanded now as a LCAO

$$\psi_i(\mathbf{r}) = \sum_j^{N_\mathrm{b}} c_{ij}\,\chi_j(\mathbf{r}), \tag{20}$$

where

$$\chi_j(\mathbf{r}) = \sum_{\mu k} w_{j\mu k}\,\varphi_{\mu k}(\mathbf{r}). \tag{21}$$

The N_b functions $\chi_j(\mathbf{r})$ are called symmetry adapted basis functions, which are formed with coefficients $w_{j\mu k}$ chosen to make the functions χ_j to transform according to the symmetry properties of the hamiltonian, i.e. according to the irreducible representations (irrep) of the point group of the hamiltonian. The number of the basisfunctions N_b should be much larger than the number of occupied orbitals N, that gives flexibility to the solutions and leads to better description of ψ_i as a linear combination of functions χ_j.

With substitutions of Eqs. 15 and 20, the Eq. 14 can be written in form of the matrix equation, or a set of s.c. secular equations,

$$\mathcal{H}\mathbf{c}_i = \varepsilon_i \mathcal{S}\mathbf{c}_i, \tag{22}$$

where the matrix elements of the hamiltonian $\mathcal{H}$ are

$$H_{mn} = \int \chi_m^*(\mathbf{r})\,h(\mathbf{r})\,\chi_n(\mathbf{r})\,d\mathbf{r} = \langle m|h|n\rangle \tag{23}$$

and those of the overlap matrix $\mathcal{S}$ are

$$S_{mn} = \int \chi_m^*(\mathbf{r})\,\chi_n(\mathbf{r})\,d\mathbf{r} = \langle m|n\rangle. \tag{24}$$

Note that

$$\langle m|h|n\rangle = \langle m|(-\frac{1}{2}\nabla_i^2)|n\rangle + \langle m|v_\mathrm{eff}(\mathbf{r})|n\rangle, \tag{25}$$

that shows how the kinetic energy contribution is calculated from those of the basis functions or atomic orbitals.

The N_b solutions, eigenvalues ε_i and eigenvectors $\mathbf{c}_i = \{c_{ij}\}$, to the matrix equation 22 are obtained through diagonalization of the hamiltonian $\mathcal{H}$. As the basis functions belong to the irreducible representations of the hamiltonian,

the matrices $\mathcal{H}$ and $\mathcal{S}$ are reduced to blocks, one for each irrep. This follows from the fact that $\langle m|h|n\rangle$ and $\langle m|n\rangle$ both vanish, if χ_m and χ_n belong to different irreps. Thus, the diagonalization can be carried out for each block independently, reducing the computational task considerably.

As mentioned above, the solutions $\mathbf{c}_i$ or ψ_i must be self-consistent. The charge density, obtained from Eq. 8 by summing over the N occupied orbitals, is responsible for the Hartree potential in Eq. 12, which is a large contribution in the effective potential, of the hamiltonian, Eq. 16. As the solutions are initially not known, the Hartree potential has to be approximated by an initial guess and then iterated until self-consistency. In practice, rather than evaluating $v_H(\mathbf{r})$ from Eq. 12 directly, it is usually solved from the Poisson equation

$$\nabla^2 v_H(\mathbf{r}) = -4\pi\rho(\mathbf{r}). \tag{26}$$

This usually results in a higher accuracy with less effort.

The above described LCAO procedure is natural and was initially developed for finite systems, molecules and clusters, with a finite number of atoms and electrons. It can be used, however, to evaluate the electronic structure of periodic bulk materials, too. A straightforward "large-cluster" model for infinite bulk always suffers from serious finite-size effects due to the cluster surface, and therefore, is not a good scheme, in general. Instead, dividing the bulk into identical computational unit cells or supercells, of which one is computed with LCAO under the explicit interaction of others, leads to better description of the periodic bulk. This kind of embedding of a supercell in between its identical images is what has been done in one of the commercially available computer codes.[21]

Although the embedding scheme is actually an application of the periodic boundary conditions, the periodicity or the full translational symmetry can not be used explicitly in defining the one-electron levels. The consequent drawback is that the wave vector (or wavelength) dependence of the computed one-electron eigenvalues is not known, and all the levels are assigned to the Γ-point (zero wave vector) of the supercell. This is also called Γ-point approximation. The quality of the solution can be increased by increasing the size of the supercell with respect to the primitive cell of the periodic bulk. This includes more one-electron levels from the Brillouin zone but in a reduced zone picture, or alternatively, it reduces the size of the first Brillouin zone, and thus, makes the Γ-point a better representative of the **k**-points in average.

3.2 Plane Wave Pseudopotential Method

The one-electron levels of a solid are delocalized and adapted to the infinite and usually periodic configuration of the component atoms, except for the deep core levels. The core levels are of less importance in cohesion of atoms and solid phase formation. Therefore, the delocalized plane waves serve as a natural and convenient basis set to expand the essential one-electron wavefunctions. The localized core levels, on the other hand, could be described only with relatively large plane wave expansions. As the main role of core electrons in this context remains their "background interaction" with the valence and conduction electrons, the ion cores can be replaced with suitable pseudopotentials with only a minor loss of accuracy in the description of delocalized levels outside the core region. A general acronym for these type of plane wave pseudopotential methods is PWPP.

Transferable core pseudopotentials are ideally constructed so, that the "scattering" properties of valence and conduction electrons, i.e. the form of of their wavefunctions, remain the same outside and become smooth and radially nodeless inside the core region. Because the scattering depends on the angular momentum of the incoming wave with respect to the nucleus, different pseudopotentials may be used for different angular momentum related quantum numbers ℓ and m_ℓ. Interactions between different ℓ channels can be included. Such a pseudopotential is called non-local and can be written in the form

$$v_{\rm pp}(\mathbf{r},\mathbf{r}') = \sum_{\mu\ell m_\ell} |\mu\ell m_\ell\rangle\, E_{\mu\ell}\, \langle\mu\ell m_\ell|', \tag{27}$$

where

$$|\mu\ell m_\ell\rangle = u_{\mu\ell}(\mathbf{r}_\mu)\, Y_{\ell m_\ell}(\hat{\mathbf{r}}_\mu), \tag{28}$$

$u_{\mu\ell}(\mathbf{r}_\mu)$ is the radial part, $Y_{\ell m_\ell}(\hat{\mathbf{r}}_\mu)$ the spherical harmonic function, $E_{\mu\ell}$ a number (energy) and μ labels the ion cores. The radial functions $u_{\mu\ell}$ and energy parameters $E_{\mu\ell}$ of pseudopotentials are fitted to suitable reference systems using various procedures.[22,27] Relativistic corrections, if essential, can easily be included into pseudopotentials, too. For more details of pseudopotentials of ion cores see Ref. 22 and references therein. Finally, the pseudopotential $v_{\rm pp}$ is added to the effective potential $v_{\rm eff}$, Eq. 16, of valence and conduction electrons.

We now consider the effects of the periodicity of the bulk lattice of atoms on the one-electron wavefunctions. Let the Bravais translation vectors defining the unit cell be $\mathbf{R}_1$, $\mathbf{R}_2$ and $\mathbf{R}_3$. This implies the periodicity of $\mathbf{R} = n_1\mathbf{R}_1 + n_2\mathbf{R}_2 + n_3\mathbf{R}_3$, where n_i are integers, in the effective potential as

$$v_{\rm eff}(\mathbf{r}+\mathbf{R}) = v_{\rm eff}(\mathbf{r}). \tag{29}$$

Now, Bloch's theorem [10] states that the one-electron eigenstates of the hamiltonian in Eq. 15 are of the form

$$\psi_{n\mathbf{k}}(\mathbf{r}) = \mathrm{e}^{i\mathbf{k}\cdot\mathbf{r}}\, u_{n\mathbf{k}}(\mathbf{r}), \tag{30}$$

where $\mathbf{k}$ is sc. wavevector, a point in the first Brillouin zone. The radius vector $\mathbf{r}$ and the wavevector $\mathbf{k}$ form a Fourier pair, the variables in space (unit cell) and in the reciprocal space (the first Brillouin zone). Thus, $|\mathbf{k}| = 2\pi/\lambda$ is proportional to the momentum of the electron wave and λ is its wavelength. Another consequence of the Fourier transform relation is the periodicity of reciprocal space, for which reason it is sufficient to consider the first Brillouin zone, only.

In Eq. 30, the one-electron eigenfunction is a product of a plane wave and s.c. cell-periodic part. The latter can be expressed further in terms of plane waves as

$$u_{n\mathbf{k}}(\mathbf{r}) = \sum_{\mathbf{G}} c_{n,\mathbf{k}+\mathbf{G}}\, \mathrm{e}^{i\mathbf{G}\cdot\mathbf{r}}, \tag{31}$$

where $\mathbf{G}$ are the reciprocal lattice vectors defined by the condition $\mathbf{G}\cdot\mathbf{R} = 2\pi m$, where m is an integer. Now, combining the two previous relations we obtain

$$\psi_{n\mathbf{k}}(\mathbf{r}) = \sum_{\mathbf{G}} c_{n,\mathbf{k}+\mathbf{G}} \exp[i(\mathbf{k}+\mathbf{G})\cdot\mathbf{r}] \tag{32}$$

for the plane wave expansion of one-electron eigenfunctions.

In an infinite solid there is an infinite number of electrons labeled with the wave vector $\mathbf{k}$. This makes the wave vector a continuous variable. On the other hand, there are more than one electronic eigenstate for each $\mathbf{k}$, labeled with the band index n above. As the eigenenergy depends on both n and $\mathbf{k}$, this results in the band structure of solids. The bands are occupied up to the Fermi energy ε_F.

It is not possible to compute an infinite number of solutions with any numerical technique. However, the eigenstates vary continuously as a function of $\mathbf{k}$, and therefore, a representative but finite set of $\mathbf{k}$-points is sufficient for an accurate description of the electronic structure. Also, the number of plane waves $|\mathbf{k}+\mathbf{G}\rangle = \exp[i(\mathbf{k}+\mathbf{G})\cdot\mathbf{r}]$ in Eq. 32 should be finite for numerical solution procedures. It is the lowest energy plane waves that are the most important in the basis set, and therefore, the basis set can be truncated to include only those plane waves who have kinetic energies $\frac{1}{2}|\mathbf{k}+\mathbf{G}|^2$ less than some particular cutoff energy. Thus, the cutoff energy describes the size of plane wave basis set and becomes a parameter that can be increased to increase the accuracy, if the available computer capacity allows.

There are a couple of more "simplifications" which we take advantage of before writing the secular equations. One is the orthogonality of plane waves, $\langle \mathbf{k}|\mathbf{k}'\rangle = \delta(\mathbf{k}-\mathbf{k}')$, that can be thought of emerging from the different translational symmetries the different plane waves represent. This is analogous with the symmetry adapted basis functions χ_j in Eq. 21, that simplified the matrix diagonalization procedure. Here, the symmetry does much better work, the hamiltonian becomes readily diagonal with respect to $\mathbf{k}$ (or kinetic energy).

The other simplification is due to the lattice symmetry, other than translational, encountered in the reciprocal lattice, too. For this reason, only one of the rotation and/or reflection related $\mathbf{k}$-points need to be considered and the solutions at the others are found using the relevant point group symmetry operations. There are methods to choose the minimal set of $\mathbf{k}$-points to represent the reduced or the whole Brillouin zone.[23]

Now, substitution of the plane wave expansion, Eq. 32, to Eq. 14 together with Eqs. 15–17 and 27 yields the matrix equation, or the s.c. secular equations,

$$\mathcal{H}\mathbf{c}_{n,\mathbf{k}+\mathbf{G}} = \varepsilon_{n,\mathbf{k}}\,\mathbf{c}_{n,\mathbf{k}+\mathbf{G}}\,. \tag{33}$$

The overlap matrix is an identity now, but for a certain $\mathbf{k}$

$$H_{\mathbf{G},\mathbf{G}'} = \frac{1}{2}|\mathbf{k}+\mathbf{G}|^2\,\delta(\mathbf{G}-\mathbf{G}') + v_{\text{eff}}(\mathbf{G}-\mathbf{G}') \tag{34}$$

and $v_{\text{eff}}(\mathbf{G})$ is defined by

$$v_{\text{eff}}(\mathbf{r}) = \sum_{\mathbf{G}} v_{\text{eff}}(\mathbf{G})\,\mathrm{e}^{i\mathbf{G}\cdot\mathbf{r}}. \tag{35}$$

The diagonalization can be carried out for each $\mathbf{k}$-point in a chosen set independently. In each case the matrix size depends on the number of included reciprocal lattice vectors $\mathbf{G}$, which further depends on the cutoff energy parameter. Here, too, the solutions have to be iterated until self-consistency.

Finally, it should be mentioned that solving the secular equations is equivalent with minimization of the total energy of the electrons, Eq. 5. Based on this there are other alternative ways of solving the electronic structure of matter, see e.g. Ref. 22. There are even straightforward methods to calculate the "molecular dynamics" of atoms simultaneously with the solution of the electronic structure and forces between the atoms.[37]

4 Surface Relaxation

The cleavage faces of binary compounds may be terminated by either of the two components. Due to the charge transfer in binding of two different elements

such a surface exposes charged surface layers and forms s.c. dipole bilayer. Such atomic scale charges effect dramatically on the physical and chemical properties of the surface. First, they create Coulomb forces between the surfacemost atomic layers that may lead to a reconstruction of the atomic geometry, or at least, to relaxation though retaining the original symmetry of the surface unit cell. Secondly, the change in chemical properties may change the nature and strength of the interactions between the surface and adsorbates, and thus, the consequent surface chemistry. Moreover, all these phenomena may further effect on the bulk properties of the material, such as the electrical conductivity, for example.

Comprehension of these phenomena motivates the detailed studies of the origins, mechanisms and consequences of the surface relaxation. In what follows, however, we concentrate more on the computational studies of these phenomena than the analysis and significance of the results and their consequences. We illustrate how the above presented methods can be applied to such investigations and compare the two different computational approaches, LCAO and PWPP.

4.1 $(10\bar{1}0)$ *Face of CdS*

Tetrahedrally coordinated compound semiconductors occur in two crystallographic allotropes: zincblende and wurtzite. Zincblende materials exhibit only (110) cleavage face but the wurtzite exhibit two cleavage surfaces: $(10\bar{1}0)$ and $(11\bar{2}0)$. All these three surfaces relax strongly resulting in deviations up the order of one Ångström from their positions in the truncated bulk geometry. There are recent reviews [4,5] of general trends and other investigations of specific cases, see Ref. 24 and references therein. The general trend in surface relaxation is anions outwards from the surface, which relates to the covalent bonding and surface electronic states. Furthermore, the surface atomic geometry is "universal" among the II–VI wurtzite semiconductors but the extent of relaxation scales linearly with the bulk lattice constant.[5]

We have chosen to consider the more general hexagonal wurtzite and the more stable of its surfaces, the $(10\bar{1}0)$. We will find that our results, like the other recent *ab initio* results [25] are in line with the general trends.

The bulk lattice parameters of the hexagonal wurtzite CdS are $a = 4.14$ Å and $c = 6.72$ Å with the c/a ratio 1.623. To be able to conveniently treat the $(10\bar{1}0)$ surface we use an orthorhombic supercell with eight atoms (two primitive cells), shown in Fig. 1. An optimization of the bulk lattice parameters with a fixed c/a ratio using total energy minimization resulted in lattice constants which deviated less than 0.1 % from the experimental ones and a very

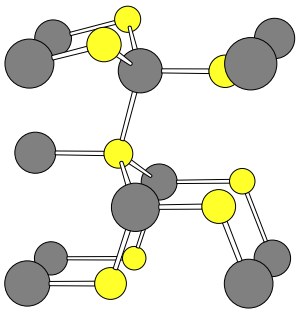

Figure 1: The orthorhombic supercell of wurtzite CdS. Smaller spheres describe anions (S) and larger cations (Cd). The upper half of the supercell illustrates the relaxed $(10\bar{1}0)$ surface but the lower half is fixed to the bulk geometry. There are eight inequivalent atoms (two primitive cells) in the corresponding bulk supercell (6.72 Å × 4.14 Å × 7.17 Å) and ten atoms in the supercell of the thinnest slab model.

small relative shift in the Cd and S lattices, with both of the computational methods. Therefore, we chose to use the experimental bulk lattice constants for the bulk and surface unit cells.

For the LCAO calculations we used a commercial software DSolid,[21] It allows self-consistent *ab initio* calculation of periodic structures with numerical atomic orbitals as a basis set, as described in Sec. 3.1. The typical extent of radial functions is 5–6 Å. For sulfur we used the following basis: $(1s^2)$, $(2s^2)$, $(2p^6)$, $3s^2$, $3p^4$, $3s^{0}*$, $3p^{0}*$, $3d^{0}*$, where those in parentheses form an atomic "frozen core" and those denoted with an asterisk have been generated in ions rather than in neutral atoms. With the same notations the basis set for cadmium is $(1s^2)$, $(2s^2)$, $(2p^6)$, $(3s^2)$, $(3p^6)$, $(3d^{10})$, $(4s^2)$, $(4p^6)$, $4d^{10}$, $5s^2$, $4d^{0}*$, $5s^{0}*$, $5p^{0}*$. Thus, the highest in energy of the inactive (frozen) set of basis functions is Cd 4p at about −65 eV (the free atom eigenvalue). The Cd 4d functions were kept active to see, if their role is important in energetics of geometric relaxation. We used the LDA parametrized by Vosko, Wilk and Nusair.[15]

For the PWPP calculations the "fhi94md" code package [26] was used. Essentially the same LDA as for LCAO was taken, but now with the Perdew-Zunger parametrization.[16] The pseudopotentials with fhi94md are of generalized norm-conserving type.[27] They consist of 1s-, 2s- and 2p-potentials for sulfur, with s being treated as a nonlocal component. The cadmium PP contains s, p and d-type functions (1s–4d) with sp-nonlocality. The number of plane waves varied from 4000 to 16000 depending on the slab thickness, as the cutoff of 10 Hartree was adopted after careful testing. For integrations over

Table 1: The perpendicular relaxation parameters of the topmost layer of wurtzite CdS $(10\bar{1}0)$ surface. Δ_{12} is the splitting of Cd and S atoms to the S and Cd layers (in Å) and ω is the corresponding rotation of the Cd–S bond from the initially horizontal direction. TB denotes tight–binding method.

CdS	Unrelaxed	LCAO	PWPP	PWPP [25]	TB [28]
Δ_{12}	0.0	0.7	0.6	0.7	0.7
ω	0°	18°	14°	16°	18°

the reciprocal space the Γ-point ($\mathbf{k} = 0$) value was taken as the representative average of the first Brillouin zone (Γ-point approximation).

The bulk supercell in Fig. 1, contains eight atoms (4 Cd + 4 S) and increase of the cell size was found to drastically increase the computational task with LCAO. With PWPP, a 16-atom (8 Cd + 8 S) supercell (two adjacent supercells of Fig. 1) was used. This was advantageous in bringing the orthorhombic cell geometry closer to cubic that was found to stabilize the internal bulk geometry very close to the experimental one. Furthermore, it increases the accuracy of the Γ-point approximation. Relaxation energies for bulk CdS with the experimental lattice constants, from the initial configuration, were 0.24 eV and 0.28 eV per primitive cell with LCAO and PWPP, respectively. The bulk relaxation results in a small relative shift of the Cd and S lattices, only.

The surface calculations were carried out with various supercell geometries. A supercell structure with four vacuum layers and four atomic layers was found to be relatively good for a quantitative description of the relaxation of the first two surface layers. The relaxed geometry is given in Table 1 together with that from the tight-binding calculations of Wang and Duke [28] and *ab initio* PWPP calculations of Schröer, Krüger and Pollmann.[25] The results from all of the calculations show a bond-length-conserving relaxation in which the top-layer cations move towards bulk and the anions move outwards from the surface plane. The rotation angle ω of the bond direction between the surface layer atoms is given in Table 1, too. The calculated relaxation is driven by the energy gain of 0.56 eV per surface unit cell according to both of our methods.

Surface densities-of-states, relevant to the chemical activity, were considered and slab models of various thicknesses were tested, too. For more details see Ref. 24.

4.2 (110) *Face of* SnO_2

The rutile crystal structure of SnO_2 is 6:3 coordinated and the bonding between atoms has a relatively strong ionic character. The (110) face is the most stable,

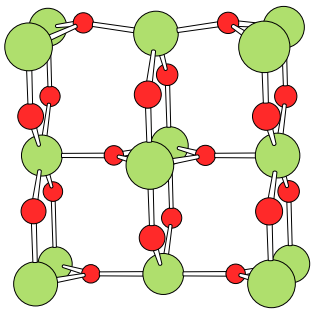

Figure 2: The orthorhombic supercell of rutile SnO_2. Smaller spheres describe anions (O) and larger cations (Sn). The upper half of the supercell illustrates the relaxed (110) surface but the lower half is fixed to the bulk geometry. There are 12 inequivalent atoms (two primitive cells) in the corresponding bulk supercell (6.67 Å × 3.19 Å × 6.67 Å) and 15 atoms in the supercell of the thinnest slab model.

and therefore, it is the most dominant surface of the crystallites of the usually porous SnO_2 material. The ideal (110) cleavage face is non-polar, but again, becomes a dipole bilayer due to the relaxation. Furthermore, the surface tends to oxidize easily, which effects on the relaxation or reconstruction, surface charge and potential, and thus, the chemical properties. Also, the oxygen vacancies present in the bulk, close to the surface and even mobile at higher temperatures interfere with the above mentioned properties.

Extensive amount of research has been done on the SnO_2 material and its surfaces both experimentally and theoretically, see Refs. 1–3, 29–31 and further references therein. Earlier, we have carried out LCAO calculations with a finite cluster model [29,30] and found out the necessity of proper embedding or inclusion of periodicity as described in Secs. 3.1 and 3.2, above. Here, we consider relaxation of the ideal (110) cleavage surface of SnO_2. This strongly relaxing face is called "reduced" in contrast to the "oxidized" surface which relaxes less.

The tetragonal unit cell contains two tin and four oxygen atoms with lattice parameters $a = 4.74$ Å and $c = 3.19$ Å. Here again we used an orthorhombic supercell with 12 atoms, shown in Fig. 2, to make calculations simpler. The same experimental lattice parameters were used throughout the study to retain simple comparability of the results from the two methods.

For the LCAO calculations the DSolid [21] software and the LDA parametrized by Vosko, Wilk and Nusair [15] were used again. For oxygen and tin we used the basis sets: $1s^2$, $2s^2$, $2p^4$, $2s^0$, $2p^0$, $3d^0$, $3d^{0*}$, and $(1s^2)$, $(2s^2)$, $(2p^6)$, $(3s^2)$, $(3p^6)$, $(3d^{10})$, $(4s^2)$, $(4p^6)$, $4d^{10}$, $5s^2$, $5p^2$, $4d^{0*}$, $5s^{0*}$, $5p^{0*}$, $5d^{0*}$, respec-

Table 2: The perpendicular relaxation parameters of the topmost layer of rutile SnO_2 (110) surface. Δ_{12} is the splitting of O and Sn atoms (average) and Δ_{11} the splitting between the two inequivalent Sn atoms (both in Å).

SnO_2	Unrelaxed	LCAO	PWPP	TB [36]
Δ_{12}	0.00	0.40	0.35	0.25
Δ_{11}	0.00	0.07	0.11	0.05

tively. The basis set notation is the same as above. The PWPP calculations were carried out with the PlaneWave software.[21,33]

Tindioxide appeared to be calculationally more demanding than CdS. The total energy minimization with PWPP led close to the experimental lattice constants only with the "extended-norm-and-hardness-conserving" pseudopotentials,[34] which required the cutoff energy of 40 Hartree (80 Ry !). The quality of the calculation was increased also by including three **k**-points for the evaluations of Brillouin zone averages. The LCAO calculations were done roughly at the same level as those for CdS. Increase of the basis set and possibly a larger supercell would have been necessary to obtain the experimental lattice constants to 1 % accuracy with LCAO. The higher demands for the calculations of SnO_2, as compared with CdS, are obviously brought by the element oxygen which is known to require not only numerically higher level calculations but also non-local corrections to LDA.

The parameters given in Table 2 describe the relaxation within the first layer of (110)-1×1 surface. They are seen to be less than those in Table 1 for CdS (roughly half). The common feature in both is, however, the anion (S or O) relaxation outwards. In case of SnO_2 the two inequivalent Sn cations relax slightly differently, too. The two methods, LCAO and PWPP, are seen to lead relatively similar relaxation, whereas the tight-binding method [36] seems to yield smaller relaxation. For more details, including supercell size effects and different slab models, see the original work.[32]

5 Conclusions

The density-functional theory is the proper framework for the *ab initio* calculation methods for solids and surfaces. It offers a straightforward formalism for numerical approaches, which become most efficient in case of large and infinite systems. Furthermore, the results are relatively accurate already at the lowest level of approximation to the exchange and correlation of electrons, the LDA, as shown in this text above. This formalism also defines the relevant concepts

for the solid state electronic structure in a simple way, and that may be more suitable even for use in qualitative molecular orbital theory of small molecules than the conventional Hartree–Fock theory, as argued in a very recent paper.[38]

Evaluation of the two different computational approaches to DFT, namely LCAO and PWPP, shows that both of them are able to describe the surface structure and properties of compound semiconductors. A reasonable accuracy can be achieved with reasonable computational efforts due to the LDA. In comparison of LCAO and PWPP the largest differences, therefore, remain in the concepts which these methods use to describe the electronic structure of periodic solids. The LCAO accounts for bonding and other phenomena in terms of atomic orbitals, whereas the PWPP emphasizes the band structure in the description of valence and conduction electrons.

As expected, the relaxation of $(10\bar{1}0)$ surface of CdS and (110) surface of SnO_2 occur essentially in the perpendicular direction, only. Lateral relaxation is negligible. Symmetry breaking reconstruction was not found, in either case. The most prominent common feature for both surfaces is the anion relaxation outwards from the surface. Various *ab initio* results for the relaxation parameters seem to mutually agree, but differ somewhat from those of tight-binding results. The extent of relaxation and the consequent effects on the surface properties are definitely essential for the adsorption and surface chemistry of these materials.

Acknowledgments

The author owes thanks his coauthors Tuomo Rantala, Vilho Lantto and Juha Vaara of the original research papers related to the work reviewed in Sec. 4, above. The Center for Scientific Computing (CSC), Espoo, Finland, is acknowledged for the computational resources and software, which have been essential for carrying out the calculations in the original work.

References

1. Vilho Lantto in *Gas Sensors*, ed. G. Sberveglieri (Kluwer Academic Publishers, Dordrecht, 1993), pp. 43–88.
2. W. Göpel, *Prog. Surf. Sci.* **20**, 9 (1985); and W. Göpel, *Microel. Eng.* **32**, 75 (1996).
3. M.J. Gillan *et al.*, *Current Opinion in Solid State & Materials Science* **1**, 820 (1996); I. Manassidis and M.J. Gillan, *Surf. Rev. Lett.* **1**, 491 (1994); I. Manassidis *et al.*, *Surf. Sci.* **339**, 258 (1995); and P.J.D. Lindan *et al.*, *Surf. Sci.* **364**, 431 (1996).

4. C.B. Duke in *Surface Properties of Electronic Materials*, eds. D.A. King and D.P. Woodruff (Elsevier, Amsterdam, 1987), Chap. 3, pp. 69–118.
5. C.B. Duke in *Reconstruction of Solid Surfaces*, eds. K. Christman and K. Heinz (Springer–Verlag, Berlin, 1990).
6. Tuomo S. Rantala, Vilho Lantto and Tapio T. Rantala, CSC News **8**, 23 (1996).
7. H.-J. Freund, *Angew. Chem. Int. Ed. Engl.* **36**, 453 (1997); and M. Bäumer, J. Libuda and H.-J. Freund in *Chemisorption and Reactivity on Supported Clusters and Thin Films*, eds. R.M. Lambert and G. Pacchioni (Kluwer Academic Publishers, Dordrecht, 1997), pp. 61–104.
8. J.C. Slater *Quantum Theory of Atomic Structure, Vols. I and II; Quantum Theory of Molecules and Solids, Vols. I and II* (McGraw–Hill, New York, 1960–1965).
9. R. McWeeny, *Methods of Molecular Quantum Mechanics*, (Academic Press, London, 1978).
10. N.W. Ashcroft and N.D. Mermin, *Solid State Physics*, (Holt–Saunders, Philadelphia, 1976).
11. P. Hohenberg and W. Kohn, *Phys. Rev.* **136**, B864 (1964).
12. W. Kohn and L.J. Sham, *Phys. Rev.* **140**, A1133 (1965).
13. R.G. Parr and W. Yang, *Density-Functional Theory of Atoms and Molecules*, (Oxford University Press, New York, 1989).
14. D.M. Ceperley and B.J. Alder, *Phys. Rev. Lett.* **45**, 566 (1980); D.M. Ceperley, *Phys. Rev.* B **18**, 3126 (1978).
15. S.H. Vosko, L. Wilk and M. Nusair, *Can. J. Phys.* **58**, 1200 (1980).
16. J.P. Perdew and A. Zunger, *Phys. Rev.* B **23**, 5048 (1981).
17. R.O. Jones and O. Gunnarsson, *Rev. Mod. Phys.* **61**, 689 (1989).
18. Tapio T. Rantala, *Acta Universitatis Ouluensis A* **184**, (1987).
19. J.P. Perdew *et. al.*, *Phys. Rev.* B **46**, 6671 (1992); and *Phys. Rev. Lett.* **77**, 3865 (1996).
20. A. Seidl *et. al.*, *Phys. Rev.* B **53**, 3764 (1996).
21. User Guides of DSolid and PlaneWave (Molecular Simulations, San Diego, 1996).
22. M.C. Payne, M.P. Teter, D.C. Allan, T.A. Arias and J.D. Joannopoulos, *Rev. Mod. Phys.* **64**, 1045 (1992).
23. H.J. Monkhorst and J.D. Pack, *Phys. Rev.* B **13**, 5188 (1976).
24. Tapio T. Rantala, Tuomo S. Rantala, Vilho Lantto and Juha Vaara, *Surf. Sci.* **77**, 352 (1996).
25. P. Schröer, P.K. Krüger and J.Pollmann, *Phys. Rev.* B **49**, 17092 (1994).
26. R. Stumpf and M. Scheffler, *Comp. Phys. Comm.* **79**, 447 (1994).

27. D.R. Hamann, *Phys. Rev.* B **40**, 2980 (1989).
28. Y.R. Wang and C.B. Duke, *Phys. Rev.* B **37**, 6417 (1988).
29. Tuomo S. Rantala, Vilho Lantto and Tapio T. Rantala, *Physica Scripta* **T54**, 252 (1994).
30. Tuomo S. Rantala, Vilho Lantto and Tapio T. Rantala, *Sensors and Actuators B* **18–19**, 716 (1994).
31. Tuomo Rantala, *Acta Universitatis Ouluensis Technica C* **96**, (1997).
32. Tapio T. Rantala, Tuomo S. Rantala and Vilho Lantto (Fourth Nordic Conference on Surface Science, May 29 – June 1, 1997 in Ålesund, Norway, Book of Extended Abstracts), eds. S. Raaen and J. Bremer, PoB-9, p. 107; and Tapio T. Rantala, Tuomo S. Rantala and Vilho Lantto, *manuscript, to be published.*
33. LDA parametrization of M.P. Teter, unpublished (1990). Similar to the parametrization of Ref. 15.
34. M.P. Teter, *Phys. Rev.* B **48**, 5031 (1993).
35. Tuomo S. Rantala, Vilho Lantto and Tapio T. Rantala, *Sensors and Actuators B* **13–14**, 234 (1993).
36. T.J. Godin, and J.P. LaFemina, *Phys. Rev.* B **47**, 6518 (1993).
37. R. Car and M. Parrinello, *Phys. Rev. Lett.* **55**, 2471 (1985).
38. E.J. Baerends and O.V. Gritsenko, *J. Phys. Chem.* A **101**, 5383 (1997).

Word index

ab initio adsorption basis function Brillouin zone catalyzed reaction CdS cleavage surface compound semiconductor configuration interaction density-functional theory exchange and correlation Fermi energy first principles Fock operator gas sensor Hartree–Fock Hartree potential LCAO linear-combination-of-atomic-orbitals local-density approximation metal oxide multiconfiguration one-electron picture plane wave pseudopotential PWPP reciprocal space rutile structure SnO_2 spherical harmonic surface diffusion tetrahedrally bonded wavefunction formalism wavevector

January 30, 1998

Contents